20. A. Qvarnström, E. Forsgren, *Trends Ecol. Evol.* **13**, 498 (1998).
21. L. Rowe, D. Houle, *Proc. Biol. Sci.* **263**, 1415 (1996).
22. M. A. Hack, *J. Insect Behav.* **11**, 853 (1998).
23. M. Zuk, L. W. Simmons, L. Cupp, *Behav. Ecol. Sociobiol.* **33**, 339 (1993).
24. W. J. Bailey, S. Haythornthwaite, *J. Zool. (London)* **244**, 505 (1998).
25. J. Hunt *et al.*, *Nature* **432**, 1024 (2004).
26. T. Tregenza, N. Wedell, *Evolution* **52**, 1726 (1998).

27. This work was supported by the Natural Environment Research Council (NERC) (grant NE/E005403/1), the NERC Sheffield Biomolecular Analysis Facility, the Leverhulme Trust, and a Royal Society Fellowship to T.T. We thank L. Rodríguez and M. C. Muñoz for providing access and facilities at the study site; J. M. López, C. López, E. González, C. R. del Valle, and F. González for assistance with the field work; and D. J. Hodgson and A. Wetherelt for assistance with data analysis and surveying.

Supporting Online Material
www.sciencemag.org/cgi/content/full/328/5983/1269/DC1
Materials and Methods
Figs. S1 and S2
Table S1
References
Movies S1 to S8

9 February 2010; accepted 12 April 2010
10.1126/science.1188102

Permissive Secondary Mutations Enable the Evolution of Influenza Oseltamivir Resistance

Jesse D. Bloom, Lizhi Ian Gong, David Baltimore*

The $His^{274} \rightarrow Tyr^{274}$ (H274Y) mutation confers oseltamivir resistance on N1 influenza neuraminidase but had long been thought to compromise viral fitness. However, beginning in 2007–2008, viruses containing H274Y rapidly became predominant among human seasonal H1N1 isolates. We show that H274Y decreases the amount of neuraminidase that reaches the cell surface and that this defect can be counteracted by secondary mutations that also restore viral fitness. Two such mutations occurred in seasonal H1N1 shortly before the widespread appearance of H274Y. The evolution of oseltamivir resistance was therefore enabled by "permissive" mutations that allowed the virus to tolerate subsequent occurrences of H274Y. An understanding of this process may provide a basis for predicting the evolution of oseltamivir resistance in other influenza strains.

Influenza A is a respiratory virus that causes annual epidemics and occasional pandemics, of which the worst on record killed in excess of 20 million people worldwide (*1*). One of the main defenses against influenza is the antiviral drug oseltamivir (Tamiflu, F. Hoffmann-La Roche, Incorporated) (*2*), and over 200 million doses have been stockpiled worldwide (*3*). Oseltamivir binds in the active site of the neuraminidase (NA) enzyme expressed on the virion surface, preventing it from cleaving sialic acid moieties that can be bound by the viral hemagglutinin protein (*2*). This lack of NA activity inhibits the release of newly formed virions from infected cells (*4*), as well as causing viral aggregation (*4*), reducing infectivity (*5*, *6*), and limiting the ability of viruses to penetrate mucus found in the airways (*6*).

During clinical testing of oseltamivir, a small fraction of human participants who were infected with the seasonal human H1N1 influenza strain A/Texas/36/1991 (TX91) and then treated with oseltamivir eventually shed resistant viruses (*7*). These viruses carried a mutation of histidine to tyrosine at NA residue 274 (H274Y), which is found near but not directly in the substrate-binding pocket (*8*). This mutation causes subtle structural alterations that weaken oseltamivir binding (*8*, *9*). However, TX91 viruses with H274Y were attenuated in tissue culture, mice, and ferrets (*10*). H274Y also impaired the growth of the H1N1 lab strain A/WSN/33 (WSN) in tissue culture (*11*) and the infectivity of the seasonal H1N1 strain A/New Caledonia/20/1999 (NC99) in ferrets (*12*). These studies led to the conclusion that "[v]irus carrying a H274Y mutation is unlikely to be of clinical consequence (*10*)."

This conclusion held sway from the introduction of oseltamivir as a drug in 1999 until the 2007–2008 influenza season, when oseltamivir-

Division of Biology, California Institute of Technology, Pasadena, CA 91125, USA.

*To whom correspondence should be addressed. E-mail: baltimo@caltech.edu

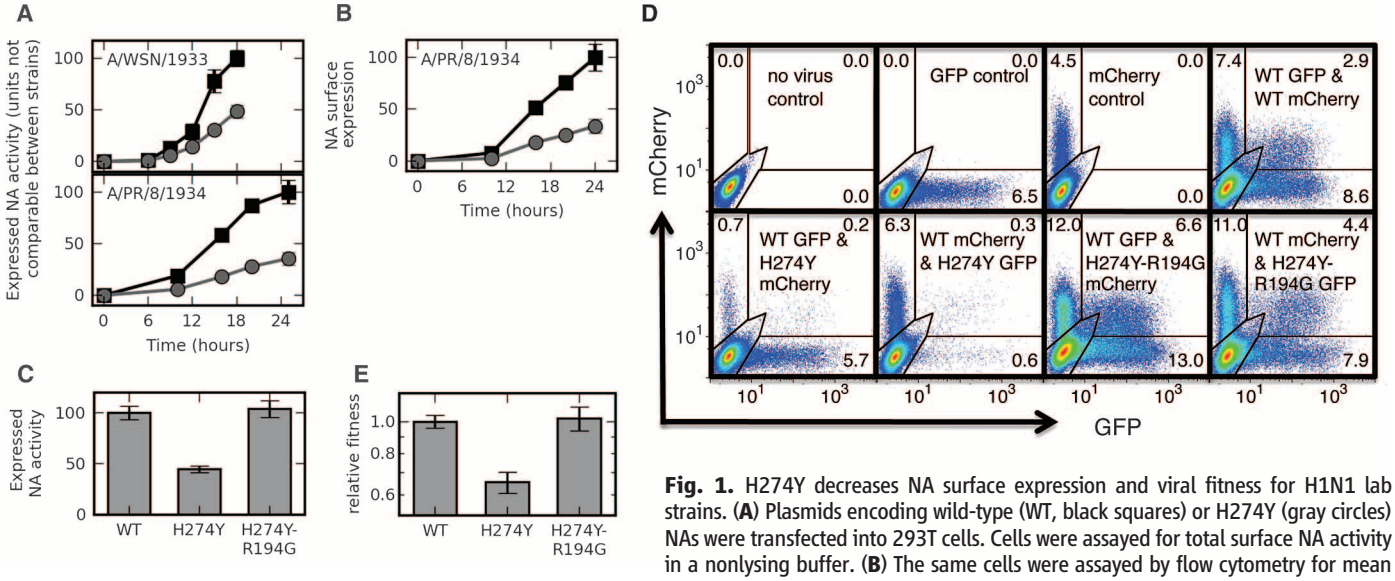

Fig. 1. H274Y decreases NA surface expression and viral fitness for H1N1 lab strains. (**A**) Plasmids encoding wild-type (WT, black squares) or H274Y (gray circles) NAs were transfected into 293T cells. Cells were assayed for total surface NA activity in a nonlysing buffer. (**B**) The same cells were assayed by flow cytometry for mean surface NA expression using a monoclonal antibody against the PR8 tetramer. (**C**) Surface activity of WT, H274Y, or H274Y-R194G WSN NA at 18 hours. All four graphs show mean ± SEM for at least three independent transfections. (**D**) An estimated 50 infectious particles of each color of WSN-PB1flank-eGFP and/or mCherry carrying the indicated NA mutations were infected into 2.5×10^5 A549-CMV-PB1 cells. After 46 to 50 hours, the cells were analyzed by flow cytometry to quantify virus growth. Numbers give percentages of cells in each gate; one representative plot is shown for each virus pair. (**E**) Relative fitness (ratio of Malthusian growth parameters) with respect to WT calculated from at least eight replicates. Shown are geometric means and 95% confidence intervals.

resistant H274Y seasonal H1N1 viruses appeared worldwide (*13*). Within a year, H274Y was present in most seasonal H1N1 (*13*). These viruses showed no obvious attenuation relative to earlier viruses carrying tyrosine at position 274 (*14*).

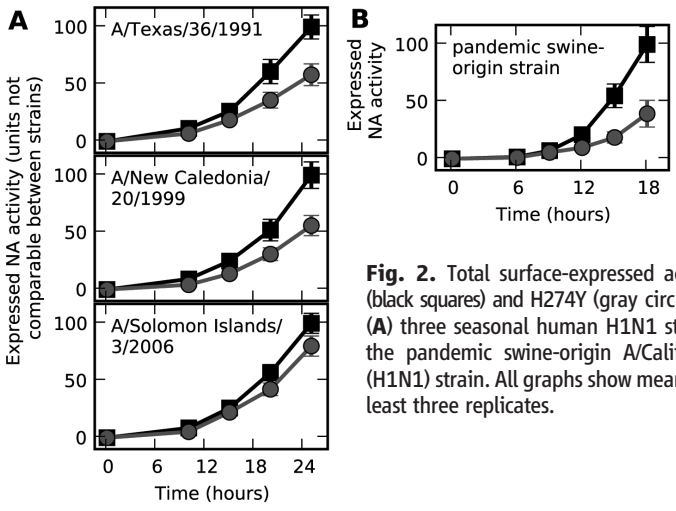

Fig. 2. Total surface-expressed activity for WT (black squares) and H274Y (gray circles) NAs from (**A**) three seasonal human H1N1 strains and (**B**) the pandemic swine-origin A/California/4/2009 (H1N1) strain. All graphs show mean ± SEM for at least three replicates.

We hypothesized that the evolution of oseltamivir resistance was enabled by permissive mutations that alleviated the deleterious effects of subsequent occurrences of H274Y. Earlier studies have failed to find large effects of H274Y on substrate affinity or catalytic rate in otherwise isogenic NAs (*9*–*11*). We therefore further hypothesized that these permissive mutations buffered previously unobserved deficiencies in NA folding or stability caused by H274Y. This hypothesis was motivated by the observation that functionally adaptive mutations often come at a cost to protein stability or folding and that mutations that bolster these properties can therefore promote evolvability (*15*).

Preliminary experiments uncovered no obvious differences in the stabilities of wild-type and H274Y NAs to irreversible thermal denaturation (fig. S1), so we examined whether H274Y hampered the efficiency with which folded NA reached the cell surface. Plasmids encoding wild-type or H274Y NA were transfected into 293T

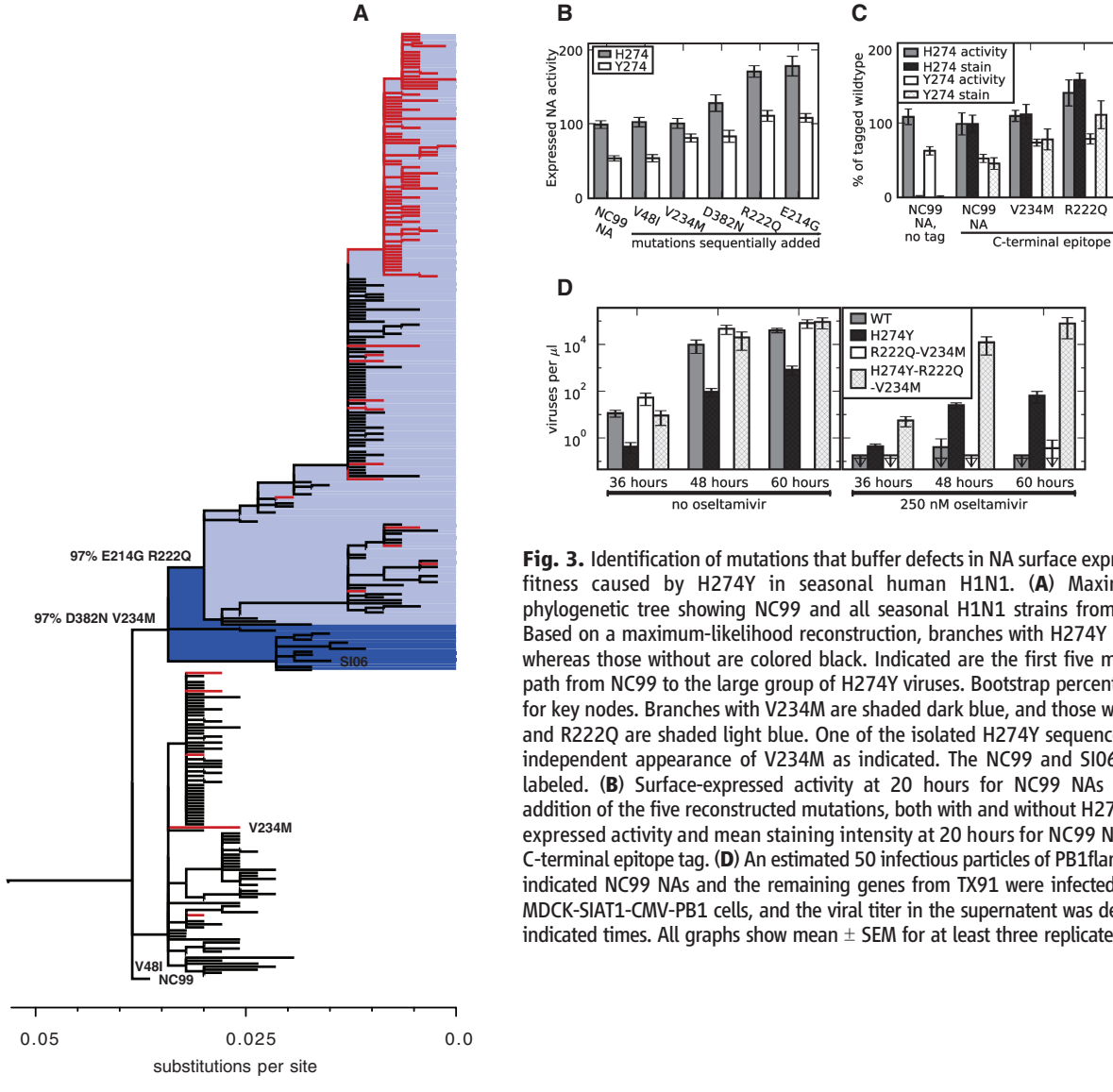

Fig. 3. Identification of mutations that buffer defects in NA surface expression and viral fitness caused by H274Y in seasonal human H1N1. (**A**) Maximum-likelihood phylogenetic tree showing NC99 and all seasonal H1N1 strains from 2006 or later. Based on a maximum-likelihood reconstruction, branches with H274Y are colored red, whereas those without are colored black. Indicated are the first five mutations on the path from NC99 to the large group of H274Y viruses. Bootstrap percentages are shown for key nodes. Branches with V234M are shaded dark blue, and those with both V234M and R222Q are shaded light blue. One of the isolated H274Y sequences contained an independent appearance of V234M as indicated. The NC99 and SI06 sequences are labeled. (**B**) Surface-expressed activity at 20 hours for NC99 NAs with sequential addition of the five reconstructed mutations, both with and without H274Y. (**C**) Surface-expressed activity and mean staining intensity at 20 hours for NC99 NAs containing a C-terminal epitope tag. (**D**) An estimated 50 infectious particles of PB1flank-eGFP with the indicated NC99 NAs and the remaining genes from TX91 were infected into 2.5×10^5 MDCK-SIAT1-CMV-PB1 cells, and the viral titer in the supernatant was determined at the indicated times. All graphs show mean ± SEM for at least three replicates.

cells, and the total NA activity expressed on the cell surface was measured by using a fluorogenic substrate (*16*). Cells transfected with wild-type NA expressed at least twofold more total surface activity than those transfected with H274Y, both for NAs from WSN and from another H1N1 lab strain, A/PR/8/34 (PR8) (Fig. 1A). Previous studies found little effect of H274Y on the catalytic activity per unit enzyme (*9*–*11*), suggesting that the differences are due to fewer NAs at the cell surface. To test this, we used a monoclonal antibody to quantify the amount of PR8 NA on the surface of transfected cells (Fig. 1B). Surface expression closely corresponded to total surface activity, confirming that H274Y decreases the amount of NA that is inserted into the membrane.

An evolutionarily important feature of mutations that interfere with protein folding is that they can frequently be compensated for by other mutations at sites distant in the three-dimensional structure (*17*, *18*). We used a computational method (*19*) to predict that Arg^{194}→Gly^{194} (R194G), which occurs over 20 Å from H274Y in the folded structure (fig. S2), might have this compensatory effect on WSN NA. Introducing R194G into H274Y WSN NA restored the total surface-expressed activity to about wild-type levels (Fig. 1C).

To examine whether a mutation that restored NA surface expression would also restore viral fitness, we created WSN viruses possessing PB1 segments in which most of the coding sequence was replaced by a gene encoding either an enhanced green or a red fluorescent protein (eGFP or mCherry) (fig. S3). Because these segments retained the noncoding and 80 terminal coding nucleotides, they were packaged efficiently and stably into virions (*20*, *21*) (fig. S3). These PB1flank-eGFP/mCherry viruses grew to high titers in cells constitutively expressing the PB1 protein. We created variants of both colors carrying wild-type, H274Y, or H274Y-R194G NAs and performed viral growth assays by adding about 50 infectious particles of each color to 2.5×10^5 A549 human lung carcinoma cells that expressed PB1 protein. After 46 to 50 hours, flow cytometry was used to quantify the cells infected by each color virus (Fig. 1D). WSN viruses with H274Y were strongly attenuated relative to wild type (Fig. 1E), in agreement with earlier work (*11*). However, H274Y virus also carrying R194G exhibited fitness indistinguishable from that of the wild type (Fig. 1E).

The foregoing results indicate that the defect caused by H274Y can be corrected by secondary mutations. To determine whether this actually occurred in human influenza, we examined NAs from seasonal H1N1. Introducing H274Y into TX91 and NC99 NAs caused an ~twofold decrease in total surface expressed activity (Fig. 2A); earlier studies have shown that H274Y attenuates these strains in ferrets (*10*, *12*). But H274Y caused a much smaller decrease in the more recent A/Solomon Islands/3/2006 (SI06) strain (Fig. 2A). We built a phylogenetic tree incorporating NC99 and all seasonal H1N1 NAs from 2006 or later (Fig. 3A) and traced along this tree from NC99 toward the large group of H274Y viruses, sequentially adding the first five reconstructed mutations in the order which maximum likelihood suggested that they occurred. Two of the reconstructed mutations had important effects on total surface-expressed NA activity (Fig. 3B). The first, Val^{234}→Met^{234} (V234M) (which is found in SI06), decreased the magnitude of the defect caused by H274Y. The second, Arg^{222}→Gln^{222} (R222Q), increased total surface-expressed activity for NAs both with and without H274Y. Both of these mutations were retained in all members of the large group of H274Y sequences (Fig. 3A). Neither mutation is in close contact with H274 in the folded NA structure (fig. S2).

To confirm that V234M and R222Q increase the amount of NA that reaches the cell surface, we added a C-terminal epitope tag. This tag was readily stained by fluorescent antibodies and did not substantially interfere with NA folding or function, because it caused at most a slight (<10%) decrease in total surface-expressed activity (Fig. 3C). Both V234M and R222Q increased the amount of NA that reached the cell surface; the activity per enzyme was unaffected by V234M and slightly decreased by R222Q (Fig. 3C). The NC99 NA carrying R222Q and V234M in addition to H274Y expressed a total surface activity roughly equivalent to that of wild type.

We next constructed PB1flank-eGFP viruses carrying NC99 NAs with the relevant mutations. The non-NA segments for these viruses were derived from the closely related (>98% protein identity) TX91 strain. We engineered a cell line (MDCK-SIAT1) that expresses high levels of the sialic acid linkage preferred by human influenza (*22*) to also constitutively express PB1 protein. We infected 2.5×10^5 cells with an estimated 50 infectious particles and monitored viral growth. The H274Y virus was strongly attenuated, growing to ~100-fold lower titers than wild type (Fig. 3D). However, virus carrying H274Y in conjunction with R222Q and V234M grew to levels comparable to that of wild type, as did virus carrying just R222Q and V234M (Fig. 3D). In the presence of 250 nM oseltamivir, only viruses carrying H274Y grew to substantial titers, with the H274Y-R222Q-V234M triple mutant growing to over 100-fold higher titers than virus with H274Y alone (Fig. 3D). Therefore, by accumulating the permissive V234M and R222Q mutations and then acquiring H274Y, NC99 virus can become resistant to oseltamivir while maintaining high levels of fitness in the absence of drug.

It is interesting to speculate about what drove the spread of these mutations in seasonal H1N1. The permissive mutations could be the result of stochastic drift, genetic hitchhiking (*23*), or selection for antigenic change or tuning of the NA/hemagglutinin balance (*24*). Once the permissive mutations were in place, H274Y could have been the product of any of these same forces or of direct selection for oseltamivir resistance. The fact that initial geographic prevalence of H274Y was not correlated with oseltamivir usage is generally viewed as evidence against direct selection for resistance (*25*), although the lack of persistent spatial structure in human influenza (*26*, *27*) makes it difficult to ascribe selection pressures to specific geographic locations.

Regardless of the forces that eventually drove its spread, our results show that H274Y attenuates seasonal H1N1 unless there are permissive secondary mutations that maintain adequate surface NA expression. These mutations likely buffer defects in NA folding or transport that are caused by H274Y. The reduced fitness of H274Y viruses in the absence of such permissive mutations could be caused by insufficient NA to balance the receptor binding of hemagglutinin (*24*) or to stimulate proper virion assembly (*28*).

The evolution of H274Y in seasonal H1N1 adds to a growing collection of examples of the importance of permissive mutations in molecular evolution. These examples include the evolution of bacterial antibiotic resistance (*29*, *30*), the escape of HIV from cytotoxic T lymphocytes (*31*), and the acquisition of new ligand specificity in vertebrate steroid receptors (*32*). An appealing aspect of our findings is that, in addition to elucidating the historic role of permissive mutations, they may also provide a basis for making informed predictions. The pandemic swine-origin 2009 A(H1N1) viruses that recently swept the globe remain mostly oseltamivir-sensitive, but scattered H274Y isolates have emerged (*33*). It remains unclear whether these isolates are less-fit evolutionary dead ends or harbingers of a resistance mutation that will soon spread worldwide. Introducing H274Y into the swine-origin A/California/4/2009 NA causes a large drop in total surface-expressed activity (Fig. 2B). We therefore suggest that, unless these swine-origin viruses already express substantial excess NA, the long-term evolutionary potential of H274Y isolates might depend on secondary mutations that rescue NA surface expression.

References and Notes

1. N. P. Johnson, J. Mueller, *Bull. Hist. Med.* **76**, 105 (2002).
2. A. Moscona, *N. Engl. J. Med.* **353**, 1363 (2005).
3. A. L. Wan Po, P. Farndon, N. Palmer, *Emerg. Infect. Dis.* **15**, 1686 (2009).
4. C. Liu, M. C. Eichelberger, R. W. Compans, G. M. Air, *J. Virol.* **69**, 1099 (1995).
5. T. Suzuki *et al.*, *J. Virol.* **79**, 11705 (2005).
6. M. N. Matrosovich, T. Y. Matrosovich, T. Gray, N. A. Roberts, H. D. Klenk, *J. Virol.* **78**, 12665 (2004).
7. L. V. Gubareva, L. Kaiser, M. N. Matrosovich, Y. Soo-Hoo, F. G. Hayden, *J. Infect. Dis.* **183**, 523 (2001).
8. R. J. Russell *et al.*, *Nature* **443**, 45 (2006).
9. P. J. Collins *et al.*, *Nature* **453**, 1258 (2008).
10. J. A. Ives *et al.*, *Antiviral Res.* **55**, 307 (2002).
11. Y. Abed, N. Goyette, G. Boivin, *Antivir. Ther.* **9**, 577 (2004).

12. M. L. Herlocher *et al.*, *J. Infect. Dis.* **190**, 1627 (2004).
13. A. Moscona, *N. Engl. J. Med.* **360**, 953 (2009).
14. M. A. Rameix-Welti *et al.*, *PLoS Pathog.* **4**, e1000103 (2008).
15. J. D. Bloom, S. T. Labthavikul, C. R. Otey, F. H. Arnold, *Proc. Natl. Acad. Sci. U.S.A.* **103**, 5869 (2006).
16. Materials and methods are available as supporting material on *Science* Online.
17. A. R. Poteete, D. Rennell, S. E. Bouvier, L. W. Hardy, *Protein Sci.* **6**, 2418 (1997).
18. A. Mitraki, B. Fane, C. Haase-Pettingell, J. Sturtevant, J. King, *Science* **253**, 54 (1991).
19. J. D. Bloom, M. J. Glassman, *PLOS Comput. Biol.* **5**, e1000349 (2009).
20. Y. Muramoto *et al.*, *J. Virol.* **80**, 2318 (2006).
21. Y. Liang, Y. Hong, T. G. Parslow, *J. Virol.* **79**, 10348 (2005).
22. M. Matrosovich, T. Matrosovich, J. Carr, N. A. Roberts, H. D. Klenk, *J. Virol.* **77**, 8418 (2003).
23. L. Simonsen *et al.*, *Mol. Biol. Evol.* **24**, 1811 (2007).
24. R. Wagner, M. Matrosovich, H. D. Klenk, *Rev. Med. Virol.* **12**, 159 (2002).
25. P. Kramarz, D. Monnet, A. Nicoll, C. Yilmaz, B. Ciancio, *Euro Surveill.* **14**, 19112 (2009).
26. M. I. Nelson *et al.*, *PLoS Pathog.* **4**, e1000133 (2008).
27. A. Rambaut *et al.*, *Nature* **453**, 615 (2008).
28. D. P. Nayak, R. A. Balogun, H. Yamada, Z. H. Zhou, S. Barman, *Virus Res.* **143**, 147 (2009).
29. X. Wang, G. Minasov, B. K. Shoichet, *J. Mol. Biol.* **320**, 85 (2002).
30. S. J. Schrag, V. Perrot, B. R. Levin, *Proc. Biol. Sci.* **264**, 1287 (1997).
31. A. D. Kelleher *et al.*, *J. Exp. Med.* **193**, 375 (2001).
32. E. A. Ortlund, J. T. Bridgham, M. R. Redinbo, J. W. Thornton, *Science* **317**, 1544 (2007); published online 16 August 2007 (10.1126/science.1142819).
33. *Wkly. Epidemiol. Rec.* **85**, 37 (2010).

34. J.D.B. was supported by a Beckman Institute Postdoctoral Fellowship and the Irvington Institute Fellowship Program of the Cancer Research Institute. L.I.G. was supported by a Summer Undergraduate Research Fellowship from the California Institute of Technology. Oseltamivir carboxylate was kindly provided by Roche.

Supporting Online Material

www.sciencemag.org/cgi/content/full/328/5983/1272/DC1
Materials and Methods
Figs. S1 to S3
Tables S1 and S2

2 February 2010; accepted 9 April 2010
10.1126/science.1187816

The Incidence of Fire in Amazonian Forests with Implications for REDD

Luiz E. O. C. Aragão[1]*† and Yosio E. Shimabukuro[2]*

Reducing emissions from deforestation and degradation (REDD) may curb carbon emissions, but the consequences for fire hazard are poorly understood. By analyzing satellite-derived deforestation and fire data from the Brazilian Amazon, we show that fire occurrence has increased in 59% of the area that has experienced reduced deforestation rates. Differences in fire frequencies across two land-use gradients reveal that fire-free land-management can substantially reduce fire incidence by as much as 69%. If sustainable fire-free land-management of deforested areas is not adopted in the REDD mechanism, then the carbon savings achieved by avoiding deforestation may be partially negated by increased emissions from fires.

Reducing emissions from deforestation and degradation (REDD) is one of the most cost-effective mitigation mechanisms (*1*) and could contribute to an emission reduction of 13 to 50 billion tons of carbon (Gt C) by 2100 (*2*). REDD is therefore a high-priority mechanism for mitigation of climate change within the United Nations Framework Convention on Climate Change (UNFCCC). The future of REDD implementation relies on forthcoming agreements to tackle the unresolved outcomes from the 15th Convention of the Parties, which took place in December 2009. These negotiations can largely influence the maintenance or replacement of the Kyoto Protocol beyond 2012 and the future of tropical forests. Policy-makers are considering a range of options for developing countries to receive financial incentives to reduce their deforestation rates (*2*). However, the efficacy of REDD as a climate change mitigation strategy depends, in particular, upon the stabilization of deforestation and degradation of the world's largest rainforest, the Amazon.

Deforestation in the Brazilian Amazon (defined as clear cutting and conversion of the original forest cover to other land uses) has resulted in annual forest area loss of 18,918 ± 1,576 km^2 (SEM) from 1998 to 2007, according to the National Institute for Space Research (INPE) in Brazil (*3*). It is estimated that this results in release of 0.28 (0.17 to 0.49) Gt C to the atmosphere annually (*4*), corresponding to 24% of the world's C emissions from land cover change [1.15 (0.58-1.79) Gt C $year^{-1}$] (*5*). In principle, discontinuing ongoing deforestation through mechanisms such as REDD would protect a large fraction of the 86 Gt of the carbon stored in Amazonian forest biomass (*6*), which is equivalent to about a decade of global fossil fuel emissions to the atmosphere. However, there is a pressing need to consider the threat to forests posed by fire.

Fires following drought years are likely to release a similar amount of carbon as emissions from deliberate deforestation (*7*, *8*). The combined effect of deliberate deforestation and forest fires has a similar magnitude to the natural annual carbon sink of 0.45 (0.3 to 0.6) Gt C estimated for undisturbed Amazonian forests (*9*). The higher probability of a drier Amazon in the 21st century predicted by some global circulation models (*10*, *11*), and consequent increasing drought intensity and frequency, may push Amazonia toward an amplified fire-prone system (*12*). Previous studies (*13*, *14*) have shown an increase in fire occurrence following two large-scale Amazonian droughts (1998 and 2005). Changes in fire frequency could jeopardize the benefits achieved through REDD; however, despite its vital importance in this region, fire is currently neglected in the emerging UN framework.

Operational satellite-derived deforestation (*3*) and fire (*15*) data sets produced by INPE, and land cover information from the European Commission's Joint Research Centre (*16*), provide a unique opportunity to quantify the sensitivity of fires to changes in deforestation rates and land use in the Brazilian Amazon. Fire in the Brazilian Amazon is likely to follow three plausible pathways: (i) Fire incidence may decrease with reduced deforestation rates by restraining human activities that are major ignition sources (*8*, *13*, *14*, *17*). (ii) It may increase even with reduced deforestation rates, both through slashing and burning of secondary forests (*18*) in already deforested areas that are not monitored by INPE's Program for Deforestation Assessment in the Brazilian Legal Amazonia (PRODES) (*19*) and through continuous enlargement of forest edges (*20*) and increasing area of secondary forest cover (*21*) that are more susceptible to fire (*22*). (iii) Fire incidence may decrease because of a shift from extensive (unmanaged) to intensive (managed) land-use methods, as the latter is normally not accompanied by deliberate use of fire (*23*).

To distinguish the first two pathways we used all available regionwide data from INPE to perform a pixel-based analysis of temporal trends in deforestation rates and fire incidence (*19*). For each pixel at 0.25° by 0.25° (or 774.35 km^2) spatial resolution, the annual fraction deforested for the period from 2000 to 2007 was derived by aggregating the 60-m spatial resolution pixels from INPE's PRODES annual deforestation maps (*3*, *19*). Similarly, the annual number of fires for each 0.25° by 0.25° pixel for the period from 1998 to 2006 was derived (*19*) by aggregating the daily

[1]Landscape and Ecosystems Dynamics Group, School of Geography, University of Exeter, Amory Building, Rennes Drive, Exeter, Devon, EX4 4RJ, UK. [2]Remote Sensing Division, National Institute for Space Research, Avenida dos Astronautas, 12227–010, São José dos Campos, São Paulo, Brazil.

*These authors contributed equally to this work.
†To whom correspondence and requests for materials should be addressed. E-mail: l.aragao@exeter.ac.uk.

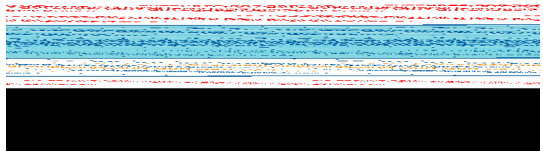

Permissive Secondary Mutations Enable the Evolution of Influenza Oseltamivir Resistance
Jesse D. Bloom, Lizhi Ian Gong and David Baltimore (June 3, 2010)

Science **328** (5983), 1272-1275. [doi: 10.1126/science.1187816]

Editor's Summary

Influenza Escape Tricks

Tamiflu, or oseltamivir, has been extensively stockpiled by several governments in anticipation of a dangerous influenza pandemic. So far, its large-scale use has not been required, but, despite this, resistance has emerged in seasonal strains mediated by a single point mutation of histidine to tyrosine in the 274 residue (H274Y) of neuraminidase. When the resistant virus was first discovered in 1998, it grew poorly, but by 2008 the virus was reinvigorated and the mutation had spread worldwide in seasonal influenza. So what happened that improved viral fitness so radically? **Bloom *et al.*** (p. 1272; see the Perspective by **Holmes**) show that the H274Y mutation hinders the folding of the neuraminidase enzyme. In the more vigorous recent oseltamivir-resistant isolates, other mutations compensate for the deleterious effect of H274Y and restore fitness to the virus.

Science (print ISSN 0036-8075; online ISSN 1095-9203) is published weekly, except the last week in December, by the American Association for the Advancement of Science, 1200 New York Avenue NW, Washington, DC 20005.